

Imaging by a phase grating used in displacement measurement

Yoichi Ohmura ^{a)}, Toru Oka ^{a)}, Toshiro Nakashima ^{a)} and Kazuhiro Hane ^{b)}

^{a)} Advanced Technology R & D Center, Mitsubishi Electric Corporation, Amagasaki, Japan

^{b)} Department of Mechanical Engineering, Tohoku University, Sendai, Japan

Abstract

Precision displacement measurement with a phase grating based on grating imaging is proposed. In this imaging system, a conventional amplitude grating as a scale is replaced by a phase grating. That generates a sinusoidal pattern, which works as an optical scale, with higher amplitude than the conventional imaging system with an amplitude grating. In this paper, analysis using an optical transfer function is described, so that optimal image contrast can be achieved. The experimental results with the image contrast of about 60 percent demonstrate good agreement with theoretical value. The results indicate the proposed method yields very good performance on displacement measurement.

Introduction

Grating imaging, used in displacement measurement, is well known [1,2]. Analyses of the grating imaging based on the optical transfer function (OTF) theory and experimental demonstration have been reported when using an amplitude grating as a pupil [3,4]. However, in amplitude grating imaging, an image contrast and received light power on an image plane, which determine accuracy and resolution in displacement measurement, were not satisfactory. In order to improve the contrast and the power, we propose using a phase grating as the pupil instead of the amplitude grating. In this paper, analysis by the OTF theory [3,4] is discussed using a phase grating with a concavo-convex shape with a 50 percent duty ratio as the pupil. To confirm theoretical results, we measured the image contrast from the intensity distribution on the image plane. Furthermore, the displacement measurement when the pupil phase grating moved was performed under high contrast imaging conditions.

Theory

The optical system of grating imaging consists of

spatial incoherent light and three planes; an object plane, a pupil plane and an image plane. The optical distribution on the object plane is imaged on the image plane by the pupil. The contrast of the image, which influences measurement accuracy and resolution, depends on the wavelength, the shapes of the pupil and the distances between three planes. To study the image contrast, OTF analysis when using a phase grating as the pupil was performed.

Figure 1 is a schematic diagram of the grating imaging system. An object grating with pitch p_1 is placed on the X_1 -axis, and illuminated by spatial incoherent light. A pupil grating with a concavo-convex shape with 50 percent duty ratio is located at a distance Z_1 from the object grating. The pitch of the pupil grating is set to p . The phase-shift amount of the pupil grating is controlled by the depth of the concavo-convex shape. The image plane is placed on the X_2 -axis located at a distance Z_2 from the pupil grating.

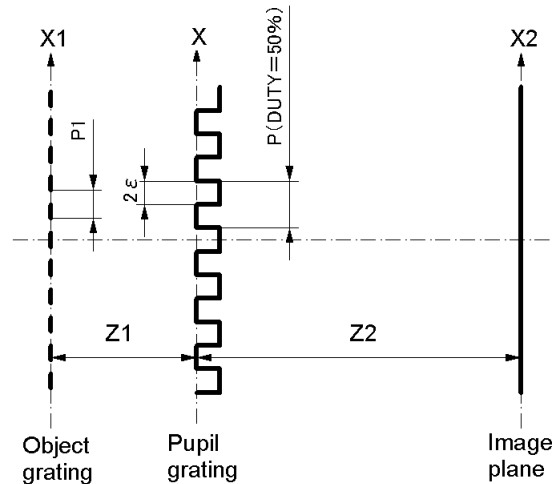


Fig.1 Schematic diagram of the optical system

The pupil function $P(x)$ of the pupil grating is defined as

$$P(x) = 1 \quad (= \exp(j0)) \quad \begin{cases} |x - np| \leq \varepsilon \\ |x - (n + \frac{1}{2})p| \leq \frac{p}{2} - \varepsilon \end{cases}$$

$$= \exp(j\theta)$$

where θ is the amount of phase-shift, 2ε is the width of its top and bottom, and n is an integer.

Generally, an OTF under incoherent illumination is defined as the Fourier transform of the square of its impulse response. In this optical system, the simplified OTF (F) in the Fresnel region can be written as

$$F(\sigma_2) = \exp\left[ika\left(\lambda^2 Z_2^2 \sigma_2^2\right)\right] \times \int P(x'-\lambda Z_2 \sigma_2) P^*(x') \exp(-2ika\lambda Z_2 \sigma_2 x') dx'$$

where $k = 2\pi/\lambda$, $a = (1/Z_1 + 1/Z_2)/2$, λ is the wavelength of the incoherent light, and $\sigma_2 (=1/P_2)$ is the image spatial frequency [3,4].

Figures 2a and 2b show the normalized OTF calculated under the $Z_1 = Z_2$ condition at $\theta = \lambda/4$ and $\lambda/2$. The horizontal axis shows the parameter $Z (=Z_1, =Z_2)$, which is normalized by $T (=P^2/\lambda)$. The parameter N describes the condition of the imaging, and is defined by the following equation.

$$\left(1 + \frac{Z_2}{Z_1}\right) \sigma_2 P = N$$

When N has an integer, the optical pattern with certain spatial frequency in the object grating is imaged on the image plane. The allowable spatial frequency is determined by the OTF as shown in Fig. 2. When Z_1 is equal to Z_2 , the allowable spatial frequency of the object and the image are the same because the magnification of this optical system is determined by the ratio of Z_1 and Z_2 . Consequently, the imaging conditions of $N = 1$ and $N = 2$ are obtained by the following configuration. For $N = 1$, the pitch of the pupil grating is set to the half of that of the object grating. For $N = 2$, the pitch of the pupil grating is equal to that of the object grating.

When θ is $\lambda/4$, the maximum absolute value, i.e. 0.637, of the OTF is obtained under the following conditions, $N = 1$ and Z is equal to the product of an odd number and T . The image inverts against the object in the location where the value of the OTF is under zero.

When θ is $\lambda/2$, the maximum absolute value, i.e. 0.637, of the OTF is obtained under the following conditions, $N = 2$ and Z is equal to the product of an odd number and $T/4$. The image contrast is two times higher than when an amplitude grating is the pupil [3,4]. In Fig. 2b, the value of the OTF is always zero when N is equal to an odd number.

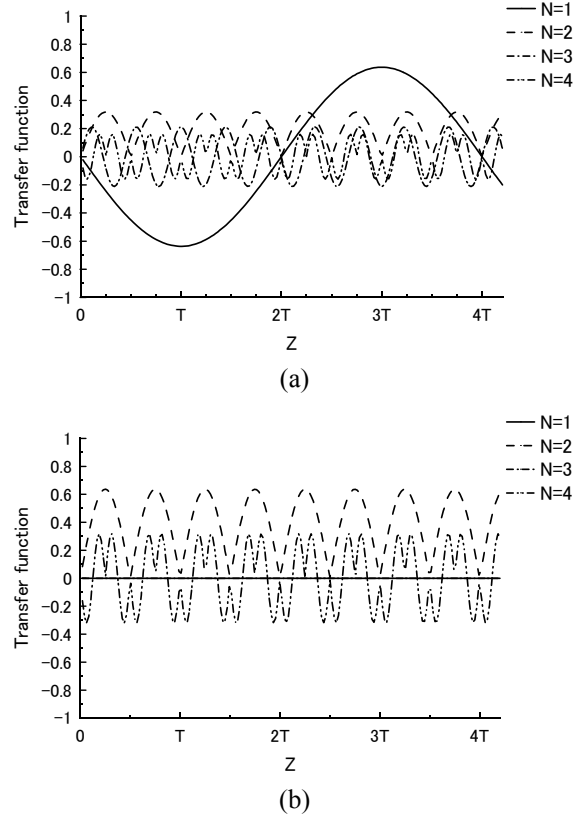


Fig. 2 Optical transfer function calculated as a function of the distance Z with allowable N , (a) $\theta = \lambda/4$ and (b) $\theta = \lambda/2$.

Experiment

Figure 3 shows the experimental setup of this optical system using the phase grating as the pupil. An infrared LED with a wavelength of 880 nm was used as the incoherent light source. The phase grating was made from a glass, and the refractive index was 1.451. The phase-shift was controlled by the depth of the concavo-convex shape. We used two phase gratings, one was 488 nm ($\lambda/4$) in depth, the other was 976 nm ($\lambda/2$) in depth. In both gratings, the duty ratios were set to 50 percent. The pitch of the phase grating when $N = 1$ and $N = 2$ were set to $P = 65 \mu\text{m}$ and $P = 68 \mu\text{m}$, respectively. The distance Z_1 between the object grating and the pupil grating was always equal to the distance Z_2 between the pupil grating and the image grating.

When $N = 1$, the pitch of the object grating and the image grating, determined by the imaging condition, were set to $130 \mu\text{m}$; this was twice as much as the pitch of the pupil grating. When $N = 2$, the pitch of the object grating and the image grating were set to $68 \mu\text{m}$ which was equal to the pitch of the pupil grating. The grating pattern of the object

grating and the image grating were made by evaporating chrome with a 50 percent duty ratio. A photodiode (PD) was placed close behind the image grating.

First, we observed the intensity distribution on the image plane without the image grating and the PD. The contrast of the intensity distribution was measured as a function of Z . Second, the output of the PD was measured when the pupil grating moved along the X -axis under high contrast imaging conditions.

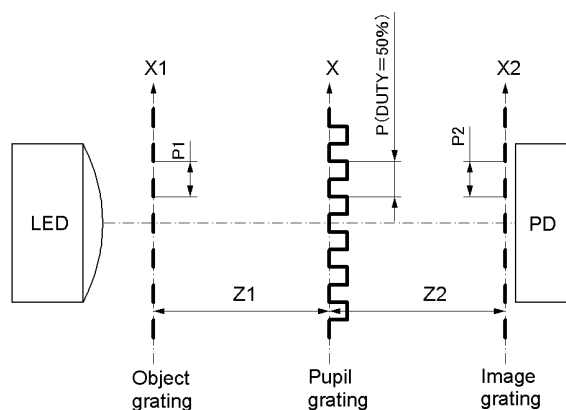


Fig. 3 Experimental setup of the optical system.

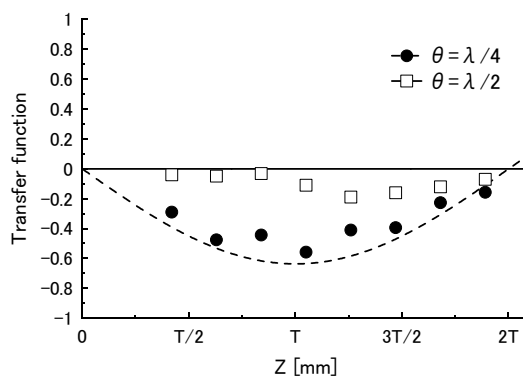
Results and discussion

Figures 4a and 4b show the experimental results of the contrast of the intensity distribution at $N = 1$ and $N = 2$. The horizontal axis shows the parameter Z normalized by T . The value of T at $N = 1$ and $N = 2$ are 4.8 mm and 5.25 mm, respectively. The solid circles and open squares show the experimental results at $\theta = \lambda/4$ and $\theta = \lambda/2$, respectively. The solid line and the broken line show the calculated results. For both $N = 1$ and $N = 2$, reasonably good agreement between the experimental results and the calculated results is apparent. When $N = 1$ and $\theta = \lambda/4$, the absolute value of the contrast was about 60 percent at $Z = T$. When $N = 2$ and $\theta = \lambda/2$, about 60 percent contrast was also obtained at $Z = T/4, 3T/4, 5T/4$ and $7T/4$. Under the $N = 2$ condition, the contrast is two times higher than that when using an amplitude grating as the pupil.

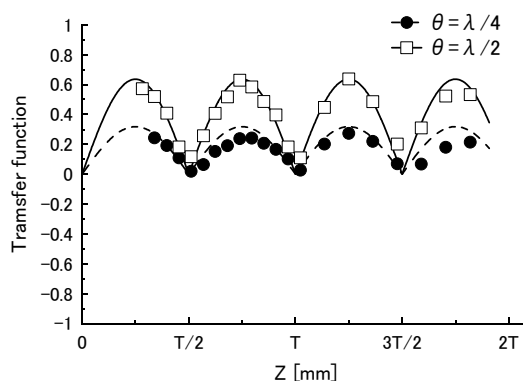
As seen in Fig. 4a, the experimental results of $\theta = \lambda/4$ are somewhat lower than the calculated result. This is caused by the harmonics included in the object grating. Compared with the calculated results of $N = 1$ and $N = 3$ in Fig. 2a, both cases have a negative value where the experimental results are lower than the calculated results in Fig. 4a.

Furthermore, the calculated results of $N = 3$ have a peak at same location. Since the third harmonic frequency ($N = 3$) and the fundamental frequency ($N = 1$) were imaged with same phase, the shape of the image resembled a rectangle wave.

To study the amplitude of the fundamental frequency directly, FFT analysis was performed on the experimental results of $\theta = \lambda/4$. Figure 5 shows the normalized amplitude of the fundamental frequency as a function of Z . The experimental results plotted as open circles come close to the calculated result. Although the experimental results from $T/2$ to T are slightly higher than the calculated results, this might be caused by the radiation characteristics of the LED.



(a)



(b)

Fig. 4 Experimental results of the OTF as a function of Z . Normalized distance T is equal to p^2/λ . (a) $N = 1$ and $T = 4.8\text{mm}$, (b) $N = 2$ and $T = 5.25\text{mm}$.

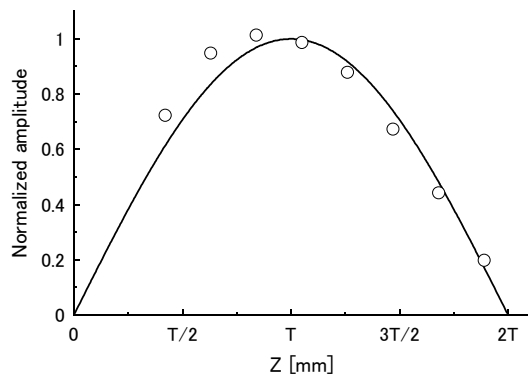
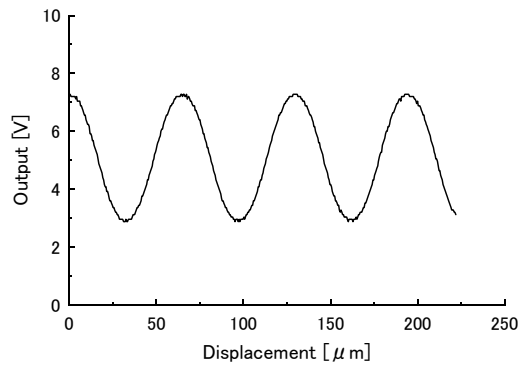
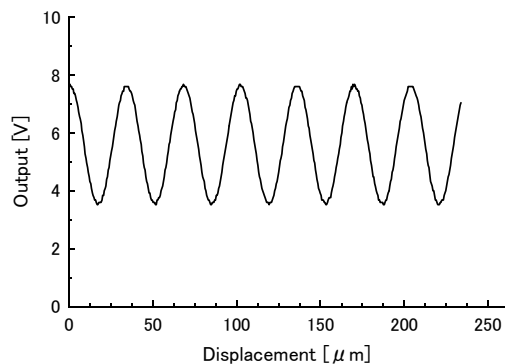


Fig. 5 The normalized amplitude of the fundamental frequency as a function of Z at $N = 1$ and $\theta = \lambda / 4$. The open circles correspond to the experimental results and the solid line shows the calculated results.



(a)



(b)

Fig. 6 Output of the PD as a function of the pupil grating displacement ; (a) $N = 1$, $\theta = \lambda / 4$, $P = 65 \mu\text{m}$ and $Z = T (= 4.8 \text{ mm})$; (b) $N = 2$, $\theta = \lambda / 2$, $P = 68 \mu\text{m}$ and $Z = 3T/4 (= 3.94 \text{ mm})$.

The output signal of the PD was measured as a function of the pupil grating displacement along the X-axis. Figures 6a and 6b show the displacement signal at $N = 1$ and $N = 2$. The displacement

measurement of $N = 1$ was done under the following conditions; the distance Z was T (4.8 mm); the depth of the phase grating was set to $488 \text{ nm} (\lambda / 4)$. The displacement measurement of $N = 2$ was done under the following conditions; the Z was $3T/4 (= 3.94 \text{ mm})$; the depth was $976 \text{ nm} (\lambda / 2)$. As shown in Fig. 6b, a displacement signal having a period equal to $34 \mu\text{m}$, which was the half of the phase grating pitch, was measured as a function of the movement of the phase grating for $N = 2$. On the other hand, the pitch of displacement signal is equal to that of the phase grating for $N = 1$. Hence, the $N = 2$ condition is better than the $N = 1$ condition with respect to the refinement of resolution.

For both $N = 1$ and $N = 2$, AC/DC ratio of about 40 percent was obtained. This value was two times higher than that with an amplitude grating as the pupil under the $N = 2$ condition. The AC/DC ratio was defined by dividing the average value into the amplitude. The received light powers of both cases were also two times higher than that with an amplitude grating because the phase grating was transparent. Finally, under the $N = 2$ condition, the amplitude of the displacement signal was four times higher than that of an amplitude grating.

Conclusion

The OTF analysis of the grating imaging when using a phase grating as a pupil was discussed. The image contrast of about 60 percent was obtained, and the received light power was twice as much as that when using an amplitude grating. The amplitude of the displacement signal was totally four times higher than that of the conventional imaging system with an amplitude grating.

References

1. R. M. Pettigrew, "Analysis of Grating Imaging and Its Application to Displacement Metrology," Proc. Soc. Photo-Opt. Instrum. Eng. 136, 325 (1977)
2. G. J. Swanson and E. N. Leith, "Analysis of the Lau effect and generalized grating imaging" J. Opt. Soc. Am. A 2, 789 (1985)
3. K. Hane and C. P. Grover, "Imaging with rectangular transmission gratings," J. Opt. Soc. Am. A 4, pp.706-711 (1987)
4. K. Hane and C. P. Grover, "Magnified grating images used in displacement sensing," Appl. Opt. 26, pp.2355-2359 (1987)